Photoluminescence from ZnS/CdS:Mn/ZnS quantum well quantum dots

L. Qian,[a] D. Bera, and P. Holloway
Department of Materials Science and Engineering, University of Florida, Gainesville, Florida 32601, USA

(Received 16 January 2008; accepted 7 February 2008; published online 3 March 2008)

Enhanced photoluminescence is reported from ZnS/CdS:Mn/ZnS quantum well quantum dots (QWQDs) prepared with a reverse micelle process. Compared to CdS:Mn/ZnS core/shell quantum dots, the QWQDs exhibited a much stronger Mn^{2+} $^4T_1$-$^6A_1$ yellow emission and the quantum yield (QY) was increased from 9% to 45%. This increased QY for QWQDs was postulated to result from the quantum well structure suppressing nonradiative relaxations from the Auger recombination at short times and reduced energy transfer between the Mn^{2+} dopants at longer times. © *2008 American Institute of Physics*. [DOI: 10.1063/1.2889446]

Quantum dots (QDs) may exhibit high quantum yields (QYs) due to strong quantum confinement.[1,2] However, QDs may still exhibit significant rates of nonradiative carrier loss due to energy transfer to surface traps and multiparticle Auger relaxation.[3] QD surfaces have been capped by organic surfactant or wide band gap inorganic shells,[4–8] leading to increased photoluminescence (PL) QYs due to suppression of nonradiative relaxation at surface states. Suppression of fast nonradiative decay due to the Auger recombination can be achieved by minimizing wave function overlap of charge carriers.[9] The Auger recombination is strongly affected by the degree of confinement and therefore was suppressed in one-dimensional CdSe quantum rods as compared to zero-dimensional QDs (Ref. 10) due to lower confinement along the dimension of the nanorod. In principle, even lower nonradiative recombination rates can be observed in two-dimensional (2D) confined layers. In one type of quantum well quantum dot (QWQD) nanostructure, a spherical QW surrounds a large band gap center core (QD) and an outer large band gap shell passivates the surface, minimizing wave function overlap in the QW. Higher efficiency PL has been reported from QWQDs, which was attributed to the pseudo-2D nature of the QW.[11]

In previous work, CdS:Mn/ZnS core/shell QDs were fabricated by a reverse micelle method.[12,13] The colloidal chemistry reverse micelle method is easy compared to the high-temperature chemical reaction method. In the case of CdS:Mn/ZnS core/shell QDs,[12,13] the ZnS shell partially suppressed the nonradiative decay processes caused by surface states, increasing the QY from ~3% to ~18%.[13] In this paper, we report on the effects of ZnS/CdS:Mn/ZnS QWQDs on PL and QY.

Both CdS:Mn/ZnS core/shell QDs and ZnS/CdS:Mn/ZnS QWQDs were produced via a reverse micelle process. In this process, $Cd(CH_3COO)_2 \cdot 2H_2O$, $Mn(CH_3COO)_2$, Na_2S, and $Zn(CH_3COO)_2$ were used as starting materials. After preparation of $(Cd^{2+}+Mn^{2+})$, S^{2-}, and Zn^{2+} aqueous solutions, each solution was stirred with a dioctyl sulfosuccinate sodium salt (AOT)/heptane stock solution, forming a stable and transparent micellar solution. The concentrations of Cd^{2+} and Zn^{2+} ions in water were $0.1M$ and $0.26M$, respectively, and the concentrations of water and AOT in heptane were $1M$ and $0.1M$, respectively. The Mn solution concentration in CdS was 4 mol %, and the molar ratio of water to surfactant was 10 for all of the $(Cd^{2+}+Mn^{2+})$, S^{2-}, and Zn^{2+} containing aqueous solutions. The CdS:Mn/ZnS core/shell QDs were prepared using the same procedure, as previously reported in Ref. 12. The QWQDs were formed by mixing 100 ml of S^{2-} and Zn^{2+} containing reverse micellar solution for 15 min. For epitaxial growth of a CdS:Mn well onto the ZnS core of the QWQD structures, ~120 ml of $(Cd^{2+}+Mn^{2+})$ containing reverse micellar solutions was added at a very slow rate into the ZnS core nanocrystal micellar solution. Subsequently, ~250 ml of Zn^{2+} containing reverse micellar solution was slowly added using a micropump. After thorough washing with heptane and methanol, the core/shell QDs and QWQDs were dispersed (stored) in methanol. A JEOL 2010F transmission electron microscope operated at 200 kV was used for imaging and direct determination of the nanocrystal size. A Perkin-Elmer PHI 5100 x-ray photoelectron spectrometer with Al $K\alpha$ x rays (1486.6 eV) was used for x-ray photoelectron spectrometer (XPS) survey scans that were collected with a step size of 0.5 eV, a dwell time of 30 ms, and a pass energy of 89.45 eV. The x-ray diffraction patterns were obtained with a Philips MRD X'Pert system. QYs were determined by comparing the integrated emission from QDs or QWQDs to that from rhodamine 6G with an excitation wavelength of 350 nm. The optical densities of the samples and reference solutions were ~0.01–0.1 at the excitation wavelength. Time-delay PL spectra were excited by the third harmonic (355 nm) of a 5 ns pulsed Quanta-Ray Nd:yttrium aluminum garnet laser running at 10 Hz.

High-resolution transmission electron microscopy (HRTEM) images of ZnS/CdS:Mn/ZnS QWQDs and CdS:Mn/ZnS core/shell QDs are shown in Figs. 1(a) and 1(b), respectively. The average size of QWQDs is ~5.7 nm, while the CdS:Mn/ZnS core/shell QDs are ~5.3 nm. We previously reported XPS and energy-dispersive spectroscopy data that were consistent with a CdS core and a ZnS shell for CdS:Mn/ZnS QDs.[12,13] XPS survey spectra from the present core/shell QDs and QWQDs are shown in Fig. 1(c). Photoelectron peaks from the Cd_{3d} and Zn_{2p} core levels are labeled and were quantitated based on the integrated peak area corrected for background and for atomic sensitivity factors. The corrected peak area ratio of Zn to Cd from the QWQDs is less than that from the core/shell structures. Since XPS is a surface-sensitive characterization technique, these data sug-

[a]Electronic mail: lqian@mse.ufl.edu.

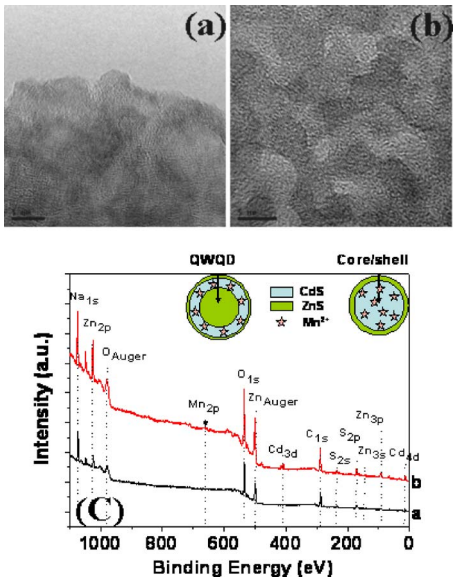

FIG. 1. (Color online) HRTEM images of Mn-doped (a) core/shell QDs and (b) QWQDs. (c) XPS survey spectra from (a) core/shell QDs and (b) QWQDs. The structures of the core/shell QDs and QWQDs consistent with the data are shown in the insets.

gest that the QWQDs have an outer ZnS shell that is thinner than the ZnS shell on the core/shell QDs. The corrected peak area ratio of Cd from the QWQD to the QDs is bigger than that of Zn, again indicating that the ZnS shell on the QWQDs was thinner than the shell on the QDs. Note that due to the low concentration of Mn (<1%), the Mn $2p$ photoelectron peak cannot be distinguished from the background noise in these survey scans.

A comparison of the PL brightness from core/shell QDs and QWQDs excited by a handheld UV lamp providing multiband irradiation between 300 and 400 nm is shown in Fig. 2(a), and emission from the QWQDs is much brighter than from the QDs. PL (350 nm excitation) and Photoluminescence excitation (PLE) (590 nm emission) spectra of core/shell QDs and QWQDs are compared in Fig. 2(b). The emission peak at ~590 nm is from the $^4T_1$-$^6A_1$ transition of Mn^{2+}. Both PL spectra have a shoulder at ~530 nm, which is stronger from the QWQDs sample. Emission at ~530 nm is also observed from ZnS/CdS/ZnS QWQDs without any dopant (not shown here). It is speculated that this PL emission results from ZnS self-activated luminescence centers, probably from vacancy and interstitial states.[14] One reason for a lower shoulder at ~530 nm from the core/shell QDs is the quenching of ZnS emission by suface nonradiative centers. In QWQDs, the surface of the ZnS core was passivated by CdS, resulting in a larger relative emission from ZnS, especially from the ZnS core.

The PLE spectra obtained by monitoring the orange emission from Mn^{2+} at 590 nm [Fig. 2(b)] show two peaks at ~325 and ~420 nm that are best associated with band absorption from ZnS and CdS, respectively. The relative intensity of the 325 nm versus the 420 nm PLE peaks is stronger for QWQDs than for core/shell QDs, indicating that a larger fraction of energy transfer in the QWQD samples was from ZnS to Mn^{2+}. This is reasonable since energy transfer only occurs over a few lattice distances; therefore, the larger interface area in QWQDs versus that in core/shell QDs leads to a larger fraction of energy transfer between ZnS and Mn^{2+}.

Time-resolved PL spectra from core/shell QDs and QWQDs after excitation by a 5 ns pulse from a 355 nm laser are shown in Figs. 2(c) and 2(d), respectively. The data show that PL emission from core/shell QDs was broad and centered at 560 nm with a shoulder at 530 nm at short times (20 ns) but narrowed and redshifted to 590 nm with time delays of 200 μs. PL emission from QWQDs was more narrow and centered at 530 nm for a delay of 20 ns and both narrowed and redshifted to 560 nm and then to 590 nm for delays of 200 ns and 200 μs, respectively. The change in shape and shift in peak wavelength with decay time both suggest that more than one transition is contributing to the PL emission. To evaluate this further, the decay of PL inten-

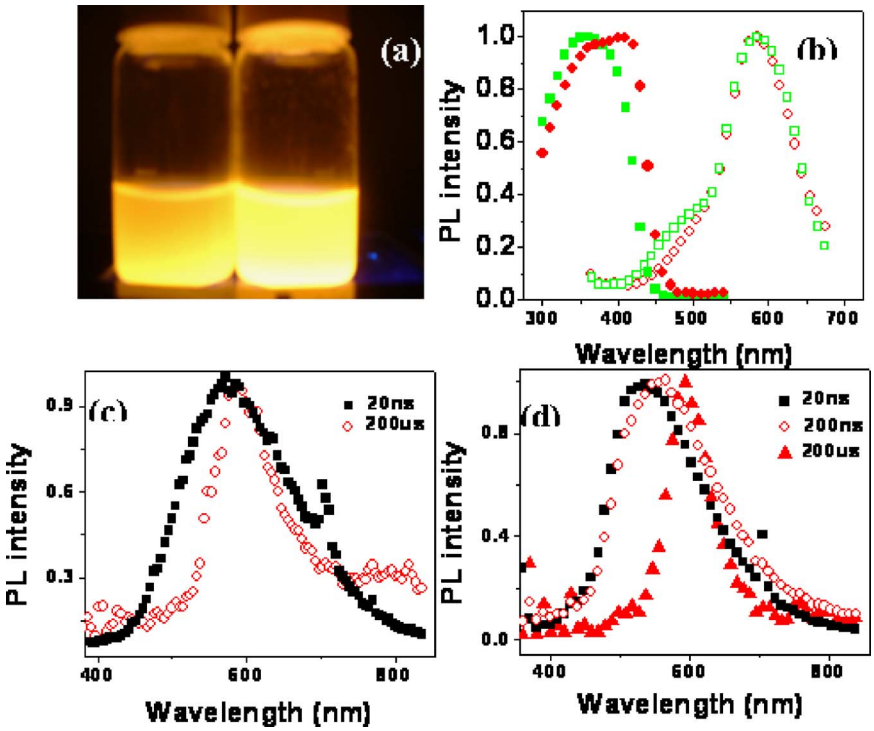

FIG. 2. (Color online) (a) Comparison of PL brightness from core/shell QDs and QWQDs excited by broad multiband (300–400 nm) UV irradiation. (b) PLE (solid; λ_{emis}=590 nm) and PLE (open; λ_{exc}=350 nm) spectra from core/shell QDs (circle) and QWQDs (square). PL spectra of (c) core/shell QDs and (d) QWQDs taken 20, 200, or 200 μs after a 355 nm excitation laser pulse.

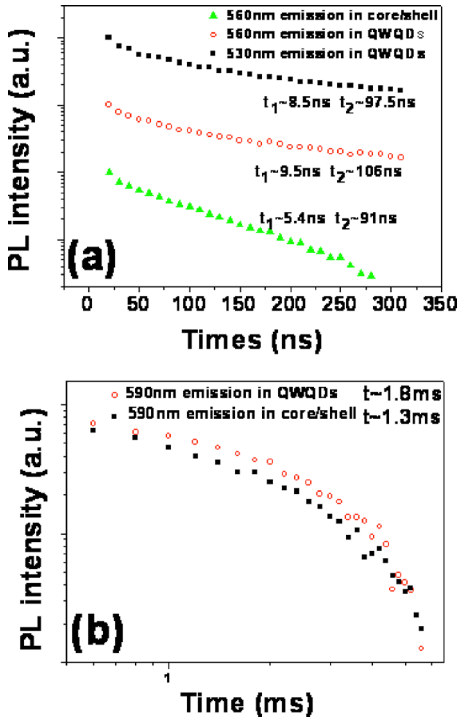

FIG. 3. (Color online) PL intensity vs time after 355 nm excitation laser pulse (a) for emission at 560 nm from core/shell QDs (▲) or emission at 530 nm (■) or 560 nm (○) from QWQDs (gate width of 10 ns, camera delay increments of 10 ns) and (b) for emission at 590 nm from either core/shell QDs (■) or QWQDs (○) (gate width of 10 μs, camera delay increments of 200 μs).

sity versus time after the excitation laser pulse was measured for core/shell QDs and QWQDs at 530 and 560 nm [Fig. 3(a)] and 590 nm [Fig. 3(b)]. As shown in Fig. 3, the PL decay data for emission at 560 nm from both core/shell QDs and QWQDs could be fitted by a biexponential curve with time constants of 91 and 106 ns, respectively. In addition, a biexponential curve was used to fit the PL decay for emission at 530 nm from the QWQDs with time constant of 98 ns. The PL decay from both core/shell QDs and QWQDs for emission at 590 nm was fitted by a single exponential decay with time constants of 1.3 and 1.8 ms, respectively. Single exponential decay is consistent with decay of the PL emission from CdS/CdSe/CdS QWQDs as reported by Xu *et al.*[15] The emissions at 530 and 560 nm from QWQDs have the same relaxation time within experimental error, suggesting that they are from the same radiative transition. Emission at wavelengths of 530–560 nm has been attributed to defect states of CdS.[16,17] Note that the lifetime of the 560 nm emission increased from 91 ns in core/shell QDs to ~106 ns in QWQDs presumably because the 2D quantum structure of the QWQD decreased the rate of competing nonradiative Auger relaxations. Similarly, the luminescent lifetime of the 590 nm emission from Mn^{2+} increased from 1.3 ms for core/shell QDs to 1.8 ms for QWQDs [as shown in Fig. 3(b)], both in the typical range of 1–2 ms for Mn^{2+} as reported by Bol and Meijerink *et al.*[18] and Smith *et al.*[19] While nonradiative Auger recombinations are expected to change the rate of radiative transitions with time constants ~100 ns, they are too fast to change the longer time constants of the $^4T_1$-$^6A_1$ Mn^{2+} transition. Instead, the increased time constants for the 590 nm emission is attributed to localization of the dopants in the QW reducing the rate of slower energy transfer processes, leading to an increased lifetime of Mn^{2+} emission. This postulate is consistent with data reported by Yang *et al.*[20] that the QY of CdS:Mn depended on whether Mn was doped in the core or in a surrounding shell. They concluded that the position dependence of the QY from Mn^{2+} was controlled by Mn–Mn interactions and local crystal field effects. For a constant dopant concentration, the Mn–Mn distance is longer in QWQDs than in core/shell QDs due to the absence of Mn at the center of the spherical core.

The passivation of surface defects by the outer shell of ZnS is as critical to QY of QWQDs as it is for core/shell QDs. Using wide band gap ZnS to confine the exciton to the CdS and reducing the rate of the Auger relaxation due to the special 2D nanostrucure in the QWQDs resulted in an increase of the PL QY of QWQDs to 45% compared to 9% for the present core/shell QDs. The PL intensities from QWQDs and core/shell QDs were not changed by storage for 3 months in room temperature laboratory air.

In summary, ZnS/CdS:Mn/ZnS QWQDs were synthesized and compared with core/shell QDs. PL QYs of 45% were obtained from QWQDs compared with 9% from core/shell QDs. The increased QY was attributed to suppression of the rates of nonradiative relaxation (Auger and energy transfer mechanisms). This postulate was supported by an increased luminescent lifetime of transitions from the pseudo-2D QW structure of the QWQDs.

This work was supported by DOE Grant No. DE-FC26-06NT42855. Assistance in data collection and reduction by Eric Lambers and Kerry Seibein of MAIC and Dr. Kirk Schanze of Department of Chemistry is gratefully acknowledged.

[1] L. E. Burs, Appl. Phys. A: Solids Surf. **53**, 465 (1991).
[2] U. Woggon, *Optical Properties of Semiconductor Quantum Dots* (Springer, Berlin, 1996).
[3] V. I. Klimov, A. A. Mikhailovsky, S. Xu, A. Malko, J. A. Hollingsworth, C. A. Leatherdale, H. J. Eisler, and M. G. Bawendi, Science **290**, 314 (2000).
[4] A. A. Bol and A. Meijerink, J. Phys. Chem. B **105**, 10197 (2001).
[5] X. Peng, M. C. Schlamp, A. V. Kadavanich, and A. P. Alivisatos, J. Am. Chem. Soc. **119**, 7019 (1997).
[6] B. O. Dabbousi, J. Rodriguez-Viejo, F. V. Mikulec, J. R. Heine, H. Mattoussi, R. Ober, K. F. Jensen, and M. G. Bawendi, J. Phys. Chem. B **101**, 9463 (1997).
[7] K. Song and S. Lee, Curr. Appl. Phys. **1**, 169 (2001).
[8] W. Jiang, A. Singhal, J. Zheng, C. Wang, and W. C. W. Chan, Chem. Mater. **18**, 4845 (2006).
[9] J. F. Xu and M. Xiao, Appl. Phys. Lett. **87**, 173117 (2005).
[10] H. Htoon, J. A. Hollingworth, A. V. Malko, R. Dickerson, and V. I. Klimov, Appl. Phys. Lett. **82**, 4776 (2003).
[11] J. Xu, M. Xiao, D. Battaglia, and X. Peng, J. Opt. Soc. Am. B **22**, 5 (2005).
[12] H. Yang and P. H. Holloway, Adv. Funct. Mater. **14**, 152 (2004).
[13] H. Yang, S. Santra, and P. H. Holloway, J. Nanosci. Nanotechnol. **5**, 1364 (2005).
[14] X. Fan, X. M. Meng, X. H. Zhang, and S. K. Wu, Appl. Phys. Lett. **86**, 173111 (2005).
[15] J. Xu, M. Xiao, D. Battaglia, and X. Peng, Appl. Phys. Lett. **87**, 043107 (2005).
[16] W. S. Chae, J. H. Ko, I. W. Hwang, and Y. R. Kim, Chem. Phys. Lett. **365**, 49 (2002).
[17] J. Zhang, L. Sun, C. Liao, and C. Yan, Solid State Commun. **124**, 45 (2002).
[18] A. A. Bol and A. Meijerink, Phys. Rev. B **58**, R15977 (1998).
[19] B. A. Smith, J. Z. Zhang, A. Joly, and J. Liu, Phys. Rev. B **62**, 2021 (2000).
[20] Y. A. Yang, O. Chen, A. Angerhofer, and Y. C. Cao, J. Am. Chem. Soc. **128**, 12428 (2006).